Virologica Sinica 39 (2024) 782–792

Contents lists available at ScienceDirect

Virologica Sinica

journal homepage: www.keaipublishing.com/en/journals/virologica-sinica
www.virosin.org

Research Article

Single-cell RNA-sequencing reveals a profound immune cell response in human cytomegalovirus-infected humanized mice

An Wang [a,b,c], Xiao-Xu Zhu [a,b,c], Yuanyuan Bie [a,b,c], Bowen Zhang [a,b,c], Wenting Ji [a,b,d], Jing Lou [a,b], Muhan Huang [a,b], Xi Zhou [a,b,c,d,*], Yujie Ren [a,b,c,*]

[a] Key Laboratory of Virology and Biosafety, Wuhan Institute of Virology, Chinese Academy of Sciences, Wuhan, 430071, China
[b] State Key Laboratory of Virology, Wuhan Institute of Virology, Chinese Academy of Sciences, Wuhan, 430071, China
[c] University of Chinese Academy of Sciences, Beijing, 100049, China
[d] School of Life Sciences, Division of Life Sciences and Medicine, University of Science and Technology of China, Hefei, 230026, China

ARTICLE INFO

Keywords:
Human cytomegalovirus (HCMV)
Single-cell RNA-Sequencing
PBMC
Viral infection

ABSTRACT

Human cytomegalovirus (HCMV) is a common herpesvirus that persistently infects a large portion of the world's population. Despite the robust host immune response, HCMV is able to replicate, evade host defenses, and establish latency throughout the lifespan by developing multiple immunomodulatory strategies, making the studies on the interaction between HCMV infection and host response particularly important. HCMV has a strict host specificity that specifically infects humans. Therefore, most of the *in vivo* researches of HCMV rely on clinical samples. Fortunately, the establishment of humanized mouse models allows for convenient in-lab animal experiments involving HCMV infection. Single-cell RNA sequencing enables the study of the relationship between viral and host gene expressions at the single-cell level within host cells. In this study, we assessed the gene expression alterations of PBMCs at the single-cell level within HCMV-infected humanized mice, which sheds light onto the virus-host interactions in the context of HCMV infection of humanized mice and provides a valuable dataset for the related researches.

1. Introduction

HCMV, a human pathogenic herpesvirus belonging to genus *Cytomegalovirus* of the *Herpesviridae* family, has a prevalence of 55%–100% within the human population. The genome of HCMV comprises double-stranded DNA (dsDNA) with approximately 230 kb in length and contains >200 predicted open reading frames, while many of them have not been found to encode proteins. Upon infection of permissive cells, HCMV genes are expressed in a tightly temporal cascade, designated immediate-early (IE), delayed early and late genes.

HCMV can establish lifelong latency after primary infection, and can be periodically reactivated when the host immune response is compromised. Most HCMV-infected individuals with normal immunity have no or mild symptoms, but immunocompromised patients, including pregnant women, newborns, organ transplant recipients, and HIV-infected individuals, may develop severe symptoms such as premature birth, abortion, neonatal congenital malformation, hepatitis, and pneumonia. In addition, HCMV infection has been reported to be closely associated with atherosclerosis, angiosarcoma, and prostate cancer.

The interaction between HCMV infection/replication and the host immune response is complex, which determines the latency/reactivation and pathogenesis of this virus, and necessitates extensive study (Fornara et al., 2022). HCMV has a strict host specificity since it only infects humans (Armstrong and Tang, 2022). This characteristics makes the humanized NOD-*scid IL2rγ*^{null} (none obesity disease/severe combined immune-deficiency/interleukin-2 receptor-γ-null) an appropriate model for studying HCMV infection, pathogenesis, and virus-host interactions in animals. Researchers had previously employed severe combined immunodeficiency (SCID) mice implanted with human fetal tissues, but these methods are labor-intensive and necessitate the use of human tissues (Bravo et al., 2007), which are hard to obtain and have lots of ethical concerns. A novel model has been developed by interbreeding NOD/SCID/IL2Rγ$^{-/-}$ mice (NSG) with NOD/SCID-SGM3 mice (*NS*-SGM). The latter expresses human cytokines SCF, GM-CSF, and IL-3.

* Corresponding authors.
E-mail addresses: renyujie@wh.iov.cn (Y. Ren), zhouxi@wh.iov.cn (X. Zhou)

https://doi.org/10.1016/j.virs.2024.08.006
Received 29 April 2024; Accepted 12 August 2024
Available online 15 August 2024

This model has proven to be effective in studying HCMV carriers in organ transplant blood and investigating the functions of HCMV proteins (Smith et al., 2010; Ren et al., 2022).

Single-cell RNA sequencing (scRNA-seq) analysis, a cornerstone of modern biological research, utilizes a spectrum of technologies for sensitive and highly multiplexed profiling, often employing combinatorial barcoding. This technology integrates single-omics methods, including genomics, epigenomics, proteomics, and metabolomics (Stuart and Satija, 2019). Traditional RNA sequencing (bulk RNA-seq) provides a mean expression profile across a multitude of cells, reflecting gene expressions of the predominant cell types. On the other hand, single-cell sequencing technologies facilitate the exploration of gene expression diversity within markedly heterogeneous samples, thereby being able to uncover complex molecular mechanisms (Liao et al., 2022; Peng et al., 2022). Current single-cell sequencing platforms combine single-cell isolation with high-throughput sequencing capabilities, enabling fast and effective characterization of extensive numbers of individual cells. An example is the 10 × Genomics system, which segregates 2000 to 20,000 cells per microfluidic channel.

As aforementioned, the interaction between HCMV and the host immune system can determine the fate of HCMV and its pathogenesis. Moreover, HCMV infection profoundly alters the host immune response, such as stimulating a substantial increase in CD8 T cell proliferation (Klenerman and Oxenius, 2016), facilitating the reconstitution of natural killer (NK) cells (Shang et al., 2023), and triggering the activation and subsequent differentiation of B cells (Zehner et al., 2023). The immune response elicited by HCMV infection is complex and involves a wide range of physiological responses. Therefore, exploring the physiological alterations of host immune system in a more precise and comprehensive way, e.g. at the level of single cells, would definitely deepen the understanding to pathogenesis and virus-host interactions of this virus. Single-cell RNA sequencing, particularly when applied to peripheral blood mononuclear cells (PBMCs), has dramatically extended the understanding of the immune system (Ramírez-Sánchez et al., 2022). PBMCs, a crucial component of the immune system, play an indispensable role in combating infections (Cho et al., 2022). And the application of scRNA-seq to PBMCs facilitates the identification and quantification of constituent cell subpopulations within a PBMC sample (Derbois et al., 2023). Previously, scRNA-seq has been applied to HCMV-infected human CD14 monocytes as a model for studying HCMV latency (Shnayder et al., 2020). However, it is unknown how HCMV infection affects the immune system in the humanized mouse model, which probably provides more knowledge in the *in vivo* context. In this study, we conducted scRNA-seq of PBMCs from HCMV-infected humanized mice, which provides a comprehensive profiling of gene expression in immune cells affected by HCMV infection.

2. Methods

2.1. Cell culture

NHDFs (normal human dermal fibroblasts) were procured from the American Type Culture Collection (ATCC). NHDFs were cultured in DMEM supplemented with 10% FBS (Gibco) and 1% streptomycin-penicillin (Gibco) at 37 °C in a CO_2 incubator.

2.2. Virus

The AD169 strain HCMV has been previously described (Ren et al., 2022). The HCMV stock was prepared on human foreskin fibroblasts (HFFs) and virus titer was determined by standard median tissue culture infective dose ($TCID_{50}$) assays. The cell-free culture supernatant was collected when the entire monolayer of HFFs was lysed.

2.3. Humanized mouse model

Human $CD34^+$ stem cell-engrafted NOD-*scid* $IL2r\gamma^{null}$ mice were purchased from Shanghai Model Organisms and housed in a specific pathogen-free (SPF) animal facility at Wuhan Institute of Virology. The animals were kept in an environment with an ambient temperature of 21 ± 1 °C, humidity of 50%–60%, and a dark/light cycle of 10/14. All animal experiments were conducted in an Animal Biosafety Level-2 laboratory that met the same housing conditions as the SPF facility. The protocols used in these experiments were approved by the Institutional Animal Care and Use Committee of Wuhan Institute of Virology. The mice were infected with HCMV by injecting 1×10^7 NHDFs intraperitoneally (i.p.). The Mock group of mice were i. p. injected with uninfected NHDFs. After four weeks, the mice were treated with 100 mL G-CSF (300 mg/mL; Amgen) and AMD-3100 (5 mg/kg) via a subcutaneous micro-osmotic pump (1007D, Alzet) for ten days to mobilize the hematopoietic stem cells. Bone marrow and spleen were collected and snap frozen for subsequent analysis after the mice were euthanized.

2.4. Isolation of PBMCs

First, blood was collected from mice using aseptic techniques and anticoagulant-containing tubes (BD vacutainer). The whole blood was transferred to a 50 mL centrifuge tube and mixed gently using a 2-fold dilution in PBS (pH 7.4, Thermo Fisher scientific 10010023). Ficoll solution (5 mL, C0025-200 ml, Beyotime) was placed in 15 mL centrifuge tube. The diluted blood was gently layered onto the upper layer of Ficoll surfacee to avoid mixing the two solutions together. The tubes were centrifuged at 800 ×*g* for 20 min, then the white cell layer was transferred to another clean 15 mL centrifuge tube with a pipette. PBS (10–15 mL) was added and tubes were centrifuged at 250 ×*g* for 10 min to remove the supernatant, and then medium was added for the same washingoperation. After separation, PBMCs were resuspended in medium (5–10 mL) for later use.

2.5. Single-cell analysis

10 × Genomics capture technology through microfluidic chips was used to detect PBMC samples for testing. For single-cell raw sequencing data, Cell Ranger software (v8.0, https://www.10 × genomics.com/support/software/cell-ranger) was employed for sequencing data quality control, barcode and UMIs splitting, and reference genome alignment. Subsequently, we generate a single-cell gene expression matrix based on cell labels and molecular labels, removing low-quality cell data. Aligning RNA reads to a reference genome using the STAR software (Spliced Transcripts Alignment to a Reference 2.7.11 b, https://github.com/alexdobin/STAR). For subsequent bioinformatics analysis, we use R Studio software (2023.12.1 + 402, https://rstudio.com/products/rstudio/download/) with the following bioinformatics analysis packages: ggplot 2, stringr, enrichplot, clusterProfiler, GOplot, and ComplexHeatmap. The cell-to-cell communication analysis were based on the CellPhoneDB database (https://github.com/ventolab/CellphoneDB).

3. Results

3.1. Sampling information for scRNA-seq

To delineate the single-cell dynamics of PBMCs during latent and reactivated HCMV infection, we procured PBMCs from the peripheral blood of human $CD34^+$ stem cell-engrafted NOD-*scid* $IL2r\gamma^{null}$ mice. These were categorized into two groups: two uninfected mice samples (Mock), and two HCMV-infected mice samples (HCMV). Initially, NHDF cells harboring HCMV were introduced into the peritoneal cavity of

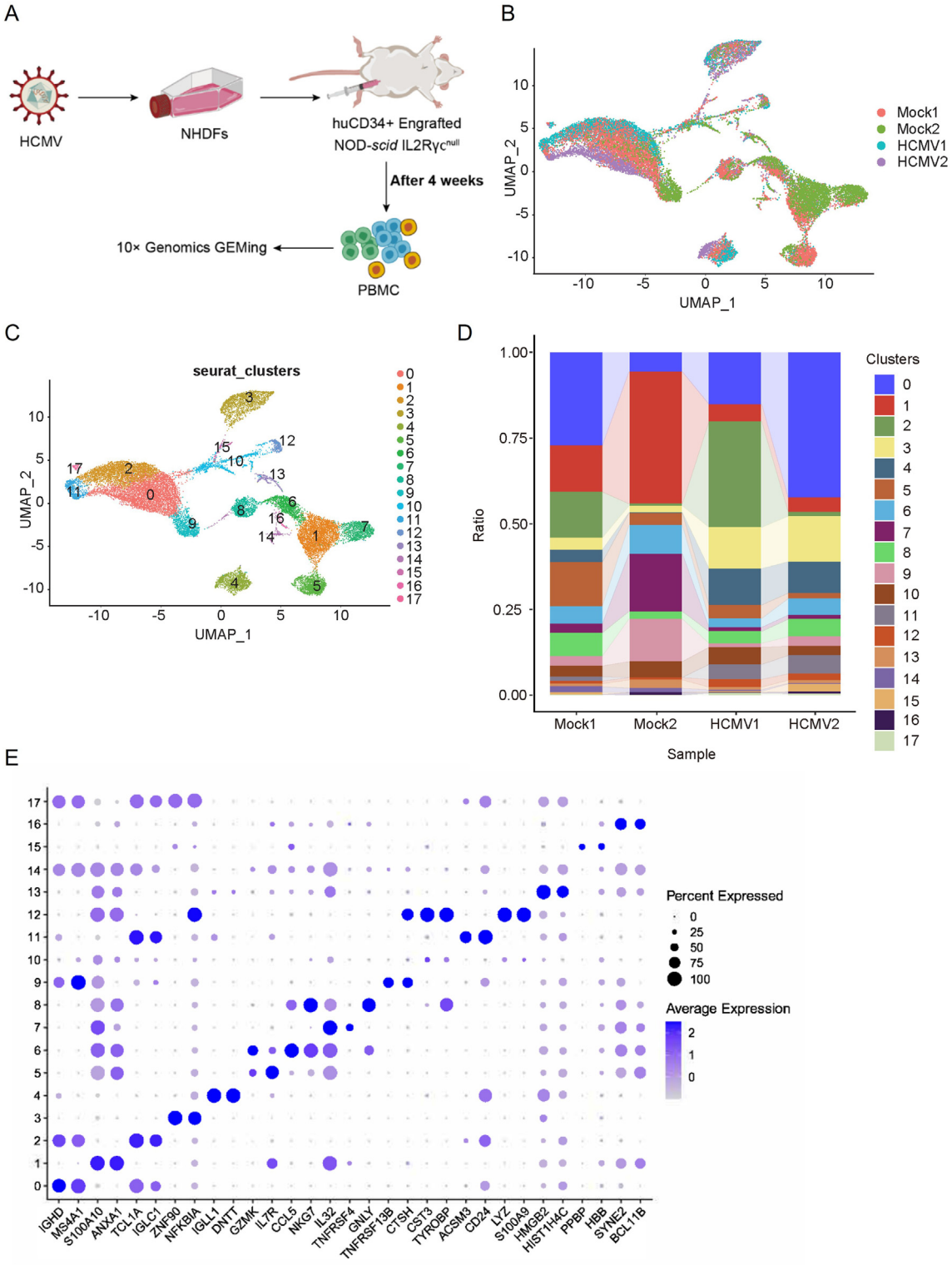

Fig. 1. Immune cell variation in HCMV-carrying humanized mice stimulated by mobilizing agents.**A** In the *in vivo* HCMV infection experiment in humanized mice, humanized NOD-*scid IL2rγ*^{null} mice were engrafted with human CD34^{+} HPCs and then transfused with NHDFs infected with HCMV. Uninfected mice served as the negative control group. At 28 days post-infection, three mice from each group were euthanized for tissue harvesting.**B** UMAP dimensionality reduction display of PBMC cell annotation results, the distribution of cell expression patterns of PBMC cells in four groups was demonstrated.**C** UMAP dimensionality reduction display of PBMC cell annotation result, The UMAP diagram shows the cell cluster analysis based on the differential expression of marker genes, with a total of 18 clusters, marked with 0–17.**D** The proportion of clusters across multiple samples is displayed as a stacked bar chart of cell proportions, the x-axis represents sample names, and the y-axis represents the proportion of cell types.**E**The gene expression levels of cells in each cluster were compared with those of the remaining cells to identify the marker gene unique to the cluster. The x-axis represents all identified differentially expressed genes, while the y-axis corresponds to marker genes. The color indicates the average expression level of marker genes in the samples, and the size of the points represents the proportion of samples expressing this marker gene.

humanized NOD-*scid IL2rγ*^{null} mice. Following a 4-week period peripheral blood was harvested and partitioned from each mouse group (Fig. 1A).

3.2. The single-cell transcriptome of PBMCs of humanized mice

For each experimental group, we isolated single cells indiscriminately of cell type and employed 10 × Genomics platforms to produce RNA-sequencing data. Initial steps included quality control of sequencing data, demultiplexing of barcodes, and Unique Molecular Identifiers (UMIs), followed by alignment to the reference genome via CellRanger software. The preliminary analysis yielded a dataset comprising 25,312 cells across four samples, encompassing two mock-inoculated controls and two HCMV-infected groups (Supplementary Table S1). Following quality control processing and data filtering on the previous dataset, we proceed with further dimensionality reduction and clustering analysis. In the gene expression data, we selectively filtered highly variable genes for downstream cell clustering analysis. Specifically, we chose the top 2000 genes with the most significant expression level changes (Supplementary Fig. S1A). In the context of each principal component (PC), we ranked them based on their contribution to the variation in cell gene expression levels. This allows us to identify the PCs that account for the majority of the variability (Supplementary Fig. S1B). We then selected the top 15 PCs for downstream dimensionality reduction analysis, and employed the Uniform Manifold Approximation and Projection (UMAP) algorithm for clustering analysis of the raw data (Supplementary Figs. S1C and S2). After that, we employed Harmony, a method for integrating and standardizing multiple single-cell datasets, for inter-sample data integration, and the UMAP plot showcases the cell clustering results for a total of four samples from the Mock and HCMV groups (Fig. 1B).

Subsequently, we performed clustering analysis on the integrated samples, resulting in the identification of 18 distinct cell clusters (Fig. 1C). Furthermore, the cell type proportions across multiple samples were visualized (Fig. 1D).

Currently, cells from different groups were subjected to clustering analysis, showing their cell type proportions. Subsequently, we conducted differential gene expression analysis at the single-cell level. Through a comparative analysis of gene expression levels between cells within each cell type (clusters) and other cell types, we identified 18 clusters based on the clustering results with res = 0.4 (Supplementary Fig. S3). For each cluster, we carefully selected the most significant marker genes and visualized gene expression differences using dot plots and UMAP graphs (Fig. 1E and Supplementary Fig. S4). Based on the annotation information from the marker genes across the 18 clusters and classic cell markers, we employed a manual annotation approach to label the cell types. Further, we have identified 15 classic cell types, such as naïve B cells, naïve CD4 T cells, progenitor natural killer (NK) cells, plasma cells, naïve CD8 T cells, natural killer T (NKT) cells, pre-T cells, NK cells, naïve immature B cells, macrophage cells, pre-B cells, classical dendritic cells (cDCs), proliferating T cells, megakaryocytes (MK) cells, and memory CD8 T cells. The cell types corresponding to each cluster and the number of cells detected are displayed in the table (Supplementary Table S2).

3.3. HCMV infection induced the humoral immunity in humanized mice

To compare the changes in the proportions of each cell type in humanized mice before and after HCMV infection, as well as the differences in gene expression at the single-cell level, we conducted a comparative analysis between the Mock group and the HCMV group. Firstly, we demonstrated the cluster analysis of 15 cell types in both groups after HCMV infection using UMAP plots, and we observed significant differences in the proportions of multiple cell types between the two groups (Fig. 2A). After HCMV infection, the proportions of the following cell types decreased: memory CD8 T cells, naïve CD8 T cells, naïve CD4 T cells, naïve immature B cells, pre-T cells, and NKT cells; in contrast, the proportions of naïve B cells, progenitor NK cells, pre-B cells, and plasma cells increased (Fig. 2B).

There is a close association between B cell development and HCMV infection. B cells exit the bone marrow and enter the bloodstream and secondary lymphoid tissues. Stimulated by CD4 T cells and dendritic cells, they become mature and undergo a series of selection and amplification processes. Ultimately, mature B cells differentiate into plasma cells that produce a large quantity of secreted antibodies or memory B cells (Kealy and Good-Jacobson, 2021). After HCMV infection, there was an increase in the proportion of pre-B cells. It has been reported that lymphoid stem cells are induced to differentiate into pre-B cells, while the proportion of naïve B cells and plasma cells also rise (Zabalza et al., 2020; Kugelberg, 2015). Thus, our observations suggest that humoral immunity became activated during viral infection. However, our data also showed that a significant proportion of key cells involved in cellular immunity was downregulated during HCMV infection. These include memory CD8 T cells, naive CD4 T cells, naïve CD8 T cells, and pre-T cells. Most of the T cell family member cells isolated from PBMCs exhibited decreased proportions in response to HCMV infection. We have also observed changes in other immune cells after infection. For instance, the proportion of progenitor NK cells increased, while NKT cell proportions decreased. Additionally, cDCs proportions increased, whereas MK cell proportions declined. Interestingly, there was no significant change observed in the proportion of macrophage cells or NK cells (Fig. 2C and D). In summary, HCMV infection in humanized mice leads to significant changes in the proportions of PBMC cells. Specifically, there was an up-regulation of cells related to humoral immunity, notably plasma cells, which directly produce secretory antibodies. Conversely, the proportions of cell types associated with cellular immunity exhibited varying degrees of decrease. These findings suggest that during HCMV infection, the humoral immunity is the major upregulated immune response in humanized mice.

3.4. HCMV infection induced profound immune cell responses in humanized mice

To assess the effects of HCMV infection on the gene expressions within each cell type, we analyzed gene expression changes in each of the 15 different cell types under infected or non-infected conditions (HCMV vs. Mock), and generated the volcano plots for multiple differential gene sets. Firstly, we aggregated the results of differential expression analysis from the 15 cell types, retaining the following labels: gene names, gene expression fold changes (Log_2FC), adjusted significance values (*P* adjust value), and cell type annotations. Based on the positive and negative Log_2FC values, we categorized genes into upregulated and downregulated groups, placing them above and below the X-axis, respectively. For each cell type, we selected the top 5 genes with the largest absolute Log_2FC values for annotation and display. Additionally, we marked genes with a *P* adjust value less than 0.01 in red, and those with a *P* adjust value greater than 0.01 in black (Fig. 3A).

To process the extensive results of differential gene analysis across the 15 cell types, we employed clusterProfiler for multi-group gene enrichment analysis. This allowed us to visualize the relationships between enriched physiological processes from Gene Ontology (GO) analysis for differentially expressed genes within these 15 cell types. The results indicate that physiological processes related to defense response to virus, regulation of innate immune response, and the viral life cycle exhibit differential expression across various cell types, including cDCs, macrophages, naïve B cells, naïve CD4 T cells, naïve CD8 T cells, naïve immature B cells, NK cells, NKT cells, plasma cells, pre-B cells, pre-T cells, and proliferating T cells. This implies that HCMV infection significantly triggered the host cell's antiviral response. Simultaneously, the virus also exploits the host's physiological processes to ensure its own life cycle (Fig. 3B).

Interestingly, physiological processes related to viral life cycle did not exhibit differential expression in memory CD8 T cells. Instead, they were

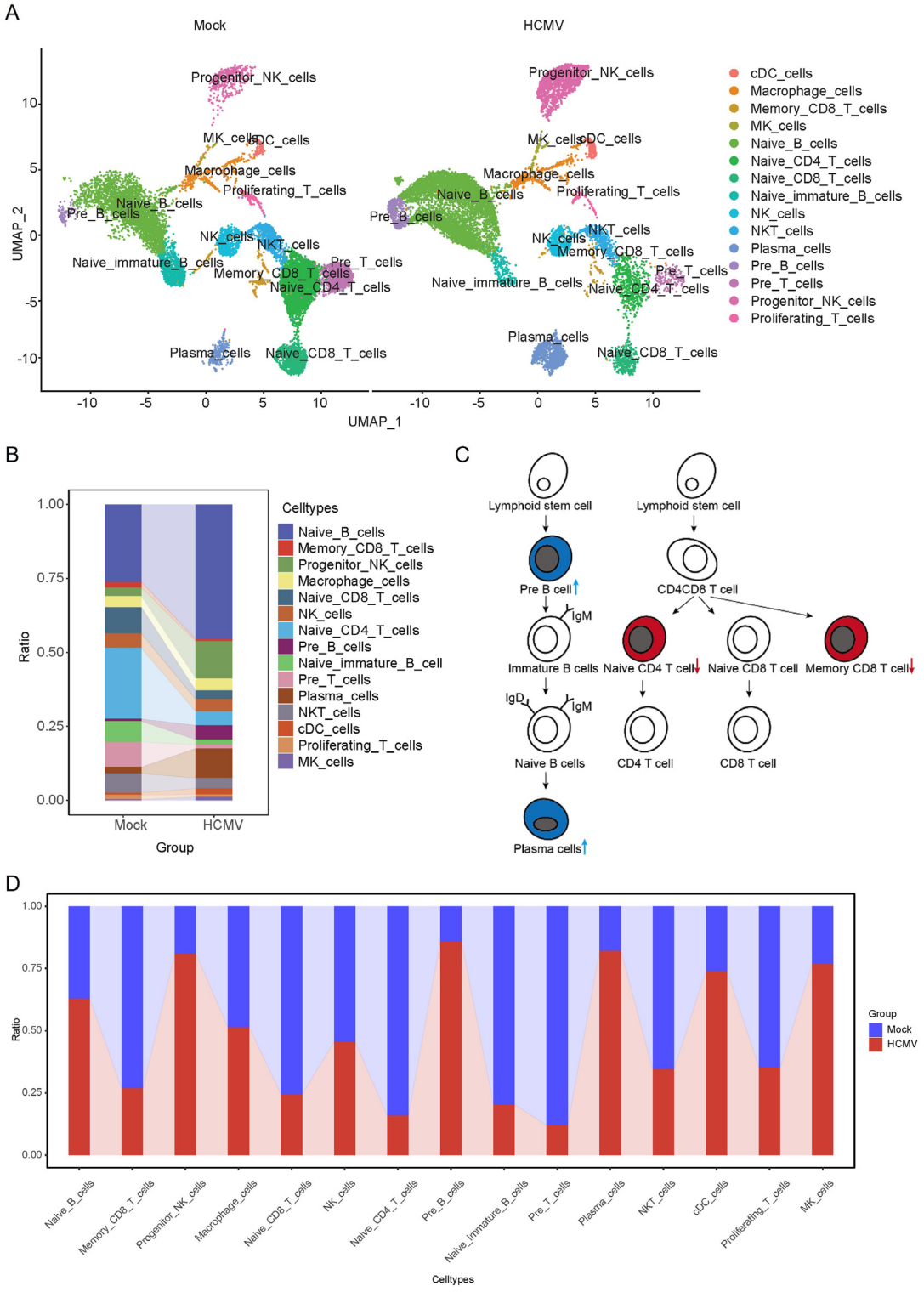

Fig. 2. Cell clustering and cell proportion analysis.**A** In the UAMP clustering analysis based on grouped samples, each point in the UMAP plot represents a cell. Points that are close together in space indicate that these cells have similar gene expression patterns. Different colors represent distinct cell types. In total, 15 cell types are displayed: naïve B cells, naïve CD4 T cells, progenitor NK cells, plasma cells, naïve CD8 T cells, NKT cells, pre-T cells, NK cells, naïve immature B cells, macrophage cells, pre-B cells, cDCs, proliferating T cells, MK cells, and memory CD8 T cells.**B** After cell annotation, the proportions of various cell clusters in individual samples and grouped samples are displayed. The x-axis represents sample names, and the y-axis represents the proportion of cell types. The specific values of the cell ratio are shown in tableS 3.**C** B cell and T cell development diagrams, and the specific changes in the proportion of cells were shown, and the data of HCMV compared with the Mock group showed that the change in the proportion of memory CD8 T cells decreased by 0.375398 times, the proportion of progenitor NK cells increased by 4.340.94 times, and the proportion of naive CD4 T cells decreased by 0.193519 times The proportion of pre-B cells increased by 6.201674 times, and the proportion of Plasma cells increased by 4.684539.**D** Proportional stacking diagram of each group of different cell types, with the abscissa being the sample name and the ordinate being the cell type ratio.

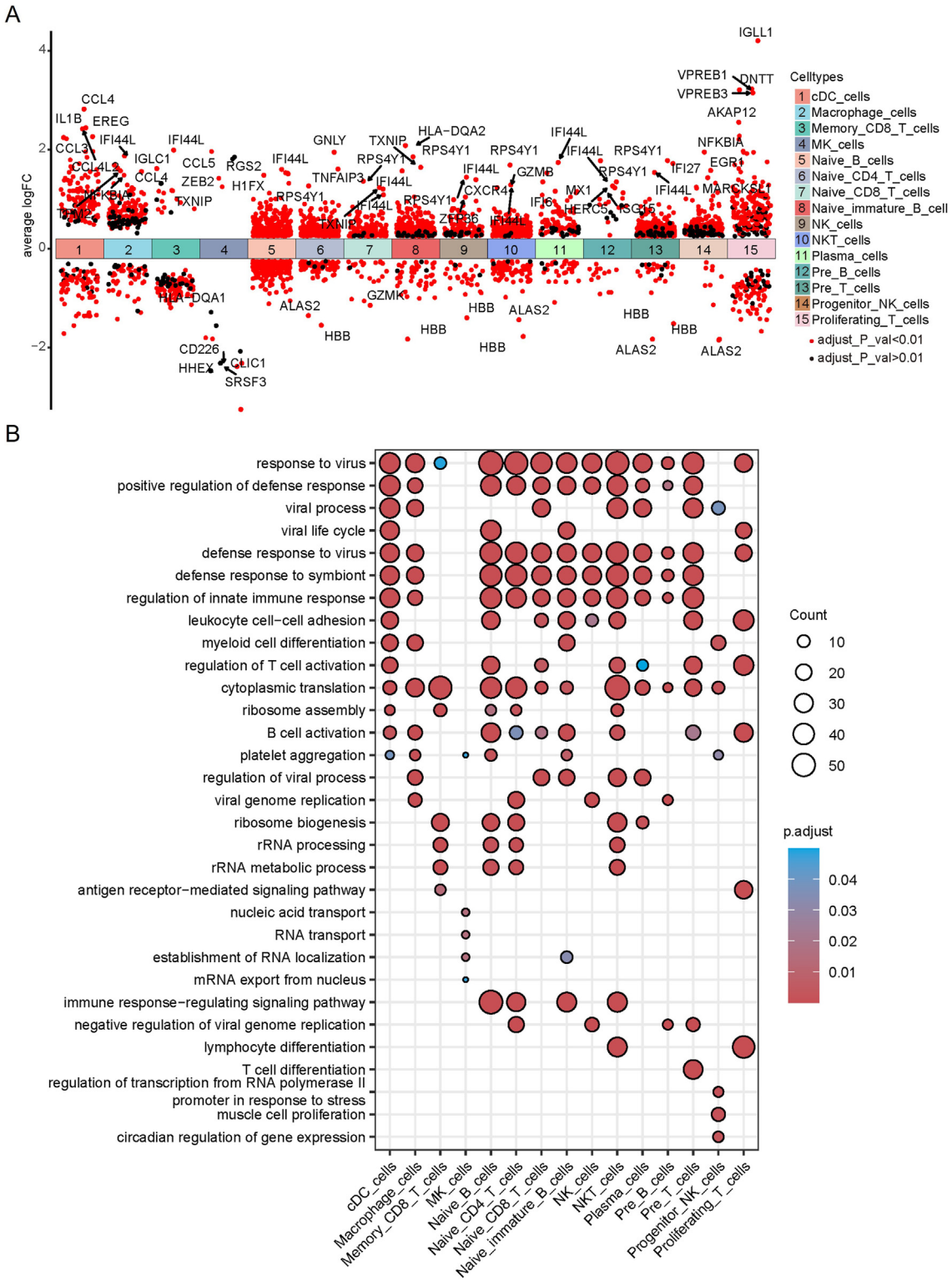

Fig. 3. HCMV infection induced the humoral immunity in humanized mice.**A** The volcano plot for multiple groups of differentially expressed genes displays various cell types on the x-axis, with each color representing a different cluster. The cell type names are listed on the right side. For each group, the plot shows the fold change in gene expression within the group. The points are differentiated based on adjusted *P*-value (red points for <0.01 and black points for >0.01). The y-axis represents gene Log_2FC (absolute value) obtained by comparing HCMV to Mock groups, and it highlights the top five genes with the largest absolute Log_2FC within each group. This visualization provides insights into significant gene expression changes across different conditions and their statistical significance. The plot was likely created using the popular R package ggplot.**B** Multiple-group enrichment analysis and visualization were performed using the clusterProfiler package in R. The dotplot function was used to visualize the results, displaying five terms. The x-axis represents cell types, while the y-axis represents the enriched biological processes. The size of the points in the plot indicates the number of genes enriched in that biological process within each cell type. The color of the points represents the adjusted *P*-value (p.adjust).

enriched in processes such as cytoplasmic translation, ribosome assembly, and rRNA processing (Fig. 3B). It has been previously reported that memory CD8 T cells are associated with chronic viral infection (Cush et al., 2007), which is consistent with our observation and suggests that the humanized mouse model can efficiently mimic the memory CD8 T cell response for HCMV infection.

In addition, the differential genes associated with physiological processes such as T cell activation, B cell activation, and leukocyte cell-cell adhesion were enriched across various cell types (Fig. 3B). This observation suggests that interactions between adaptive immune cells play a crucial role during HCMV infection. Further study is needed to explore the intricate relationships between these immune components.

Together, our findings indicate that HCMV infection induced profound immune cell responses in humanized mice, which should resemble the *in vivo* responses induced by authentic HCMV infection.

3.5. Antiviral genes showed significant changes in the upregulated cell types

In order to investigate the typical antiviral processes in PBMCs at the genetic level, we conducted GO analysis on the group with significantly upregulated cell proportions during HCMV infections (Supplementary Fig. S5A). The results showed that in the plasma cells, numerous interferon-stimulated genes (ISGs) were significantly upregulated, which include *IFI44*, *IFI6*, *IRF7*, *IFIT3*, *IFI44L*, and *ISG20*. These ISGs play crucial roles in host's natural immune response against viral infections. Additionally, genes such as *EIF2AK2*, *OAS1*, *MX1*, *IFITM3*, *ISG20*, *STAT1*, *OAS3*, and LY6E, which are involved in regulating gene expression levels during the virus infection process and life cycle, were also upregulated (Fig. 4A and Supplementary Fig. S6). In the pre-B cells, the genes *OAS1*, *OAS2*, *MX1*, *ISG15*, *EIF2AK2*, and *PLSCR1* were upregulated after HCMV infection, and they simultaneously participate in regulating the virus life cycle and antiviral physiological processes. On the other hand, *IFI44L* and *IRF7*, as well as *HERC5*, were upregulated after infection and directly contribute to the antiviral response (Fig. 4B and Supplementary Fig. S7). These observations indicate that plasma cells and pre-B cells, upon be infected by HCMV, dramatically increase the expression of ISGs and other antiviral genes, leading to the activation of antiviral immunity, which highlights the role of B cells in combating against HCMV infections.

Progenitor NK cells, following HCMV infection, significantly downregulated the expression of *EGR1*, *ATF3*, and *CITED2* genes, but upregulated the expression of *JUN*. These genes primarily participate in the transcriptional regulation of DNA and RNA. Simultaneously, among the genes associated with cellular homeostasis, *ID2* (involved in negative regulation of cell differentiation), *PDE4B*, *NFKBIZ*, *TNFAIP3*, *SKIL*, *HMGB2*, and *CITED2* were downregulated, whereas *ALAS2*, which catalyzed mitochondrial heme synthesis, was significantly upregulated. Additionally, genes related to extrinsic apoptosis signaling pathways, including *ATF3*, *HMGB2*, *TNFAIP3*, and *SKIL*, were downregulated. Furthermore, cell proliferation-related genes were downregulated, while mitochondrial energy synthesis-related genes were upregulated, providing a plausible explanation for the increased proportion of progenitor NK cells after HCMV infection (Fig. 4C and Supplementary Fig. S8).

In summary, during HCMV infection, the proportions of plasma cells, pre-B cells, and progenitor NK cells were upregulated, and the antiviral genes were significantly increased in these cells.

3.6. HCMV infection decreased the proportion of memory CD8 T cells and naïve CD4 T cells

We then focused on the two cell types that exhibited a significant decrease in proportion in response to HCMV infection, i.e. naïve CD4 T cells and memory CD8 T cells. We conducted GO analysis on these cell types (Supplementary Fig. S5B). Memory CD8 T cells play a crucial role in adaptive immunity, providing rapid responses upon antigen stimulation. In the GO analysis, we observed downregulation of genes related to cytoplasmic translation and RNA transcription in memory CD8 T cells following HCMV infection. The ribosomal protein family members RPL and RPS were significantly enriched and their gene expression levels were markedly downregulated, suggesting a decrease in intracellular protein synthesis. Simultaneously, the expression of molecular chaperones HSP90AA1 and HSP90AB1 was also downregulated, along with the expression of TRMT122, which is involved in protein modification and RNA processing. These observations indicate an overall reduction in protein synthesis in the memory CD8 T cells, probably caused by HCMV infection (Fig. 5A and Supplementary Fig. S9).

Naïve CD4 T cells are found in lymph nodes and serve as sentinels, monitoring MHC molecules. Upon activation by antigen-presenting cells, they can rapidly differentiate into either effector T cells or regulatory T cells. The GO analysis revealed that differentially expressed genes in naïve CD4 T cells were primarily enriched in physiological processes related to antiviral responses and the regulation of antiviral pathways. For instance, the expression level of the DEAD-BOX RNA helicase DDX60 was upregulated, along with the increased expression of classic ISGs such as *IFI44L*, *IFI6L*, and *IFIT3*, as well as *HERC5*, an E3 ligase for ISG15 (Fig. 5B and Supplementary Fig. S10). This indicates that the expression levels of certain genes involved in regulating host innate immunity are upregulated in naïve CD4 T cells, while the proportion of these cells were decreased.

3.7. HCMV infection enhanced cell-to-cell communications in humanized cells

Cell-to-cell communication, mediated by ligand-receptor complexes, is crucial for coordinating diverse biological processes, including development, differentiation, and inflammation. CellPhoneDB, a novel database, focuses on ligands, receptors, and their interactions. It is built on the premise that complex extracellular reactions originate from ligand binding to their cognate receptors, and triggering specific cell signaling pathways. To analyze the impact of HCMV infection on cell-to-cell communications, we calculated the *P*-value for a specific interaction pair using a permutation test. First, we randomly shuffled the cell type labels and computed the average expression level for the interaction. This process was repeated 1000 times to obtain the distribution of average expression levels. Next, we identified the top 50 expression values that exceed the average distribution. These were considered significant, with a *P*-value less than 0.05 (50/1000). Using the CellPhoneDB, we analyzed cell communication within the sample, resulting in an intercellular interaction network between different cell types (Fig. 6A). For ease of the presentation, we tabulated the number of interactions between paired cell types and visualized them as a heatmap (Fig. 6B). The results indicate a substantial enhancement of cell-to-cell communication in immune cells within PBMCs following HCMV infection. Notably, there was increased interaction between cDCs and other immune cell types. This finding suggests that this specialized antigen-presenting cell type significantly enhances its major histocompatibility complex (MHC) peptide presentation function after HCMV infection. This enhanced function is closely linked to the activation and differentiation of naïve T cells and the maturation of B cells. Furthermore, the immune microenvironment in the blood becomes activated after HCMV infection, leading to antiviral responses, host immune regulation, and upregulation of genes involved in protein synthesis. These dynamic changes are also reflected in the CellPhone, which captures intercellular communication patterns. Unlike most immune cells, some other cell types, such as MK cells that primarily function in platelet production within the bone marrow, were minimally affected by HCMV infection in terms of cell-to-cell communication. This observation suggests that HCMV infection primarily triggers reprogramming of the immune microenvironment (Fig. 6B).

Therefore, during HCMV infection, there is a significant increase in cell-cell interactions among different cell types within PBMCs. This phenomenon explains the high enrichment of differentially expressed genes related to T cell activation, B cell activation, and leukocyte cell-cell adhesion observed in the GO analyses. Specifically, the increased

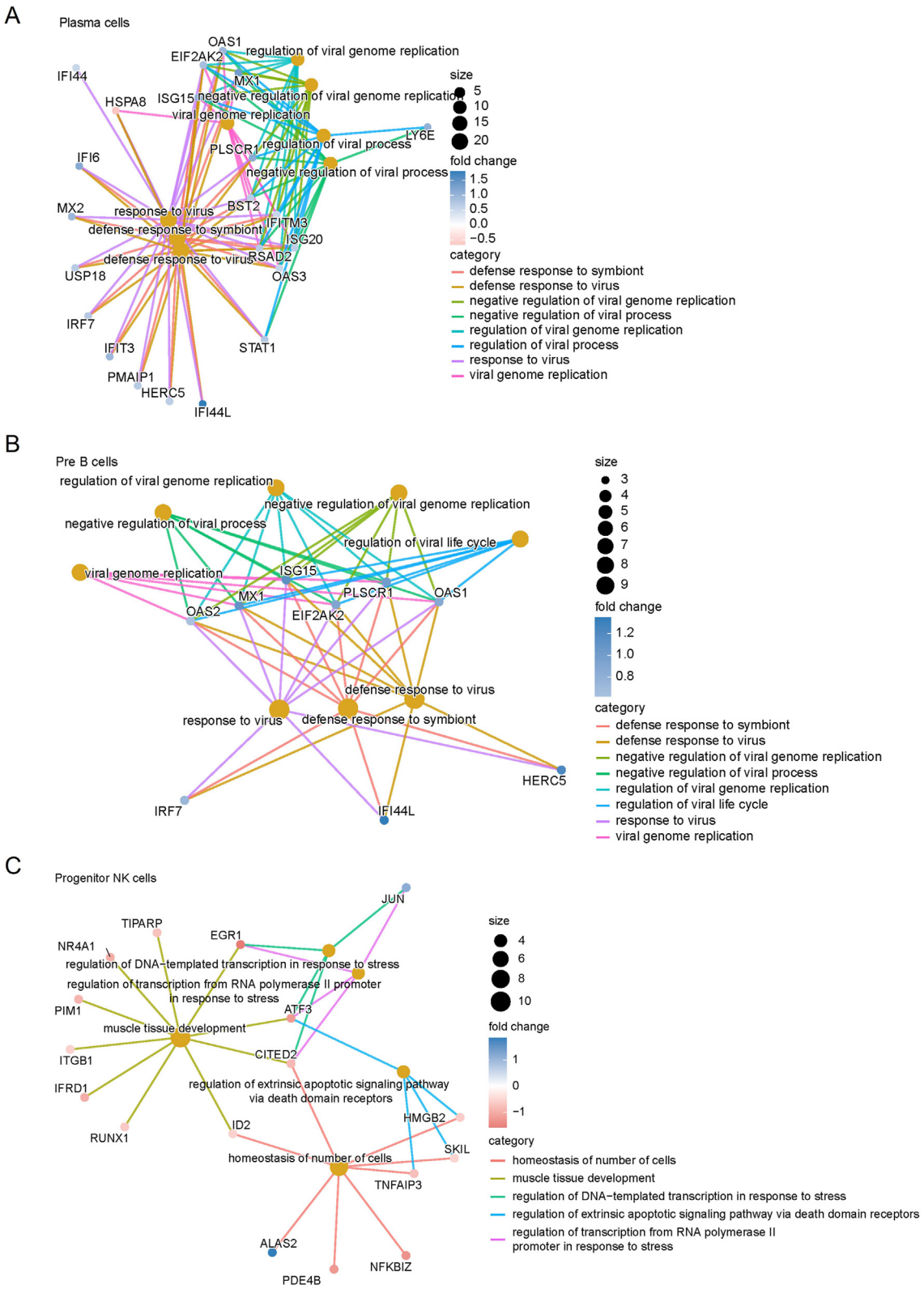

Fig. 4. Antiviral genes showed significant changes in the upregulated cell types. Plasma cells, pre-B cells, progenitor NK are demonstrated The GO enrichment analysis of differential genes in the HCMV group of cells compared with the Mock group was analyzed by using clusterprofiler software to analyze the enrichment of a gene to the most significant eight GO terms and plotted a cnetplot plot to display, the yellow dots in the graph are GOterm, the dot size represents the number of genes, the lines of different colors represent different categories, the nodes represent genes, and the color shade indicates the size of gene expression changes. **A, B** enriched into eight GO terms, namely: defense response to symbionts, defense response to virus, negative regulation of viral genome replication, negative regulation of viral processes, regulation of viral genome replication, regulation of viral processes, response to viruses, and viral genome replication. **C** Enriched into eight GO terms, namely: defense response to symbionts, defense against viruses, negative regulation of viral genome replication, negative regulation of viral processes, regulation of viral genome replication, regulation of viral life cycle, response to viruses, and replication of viral genomes.

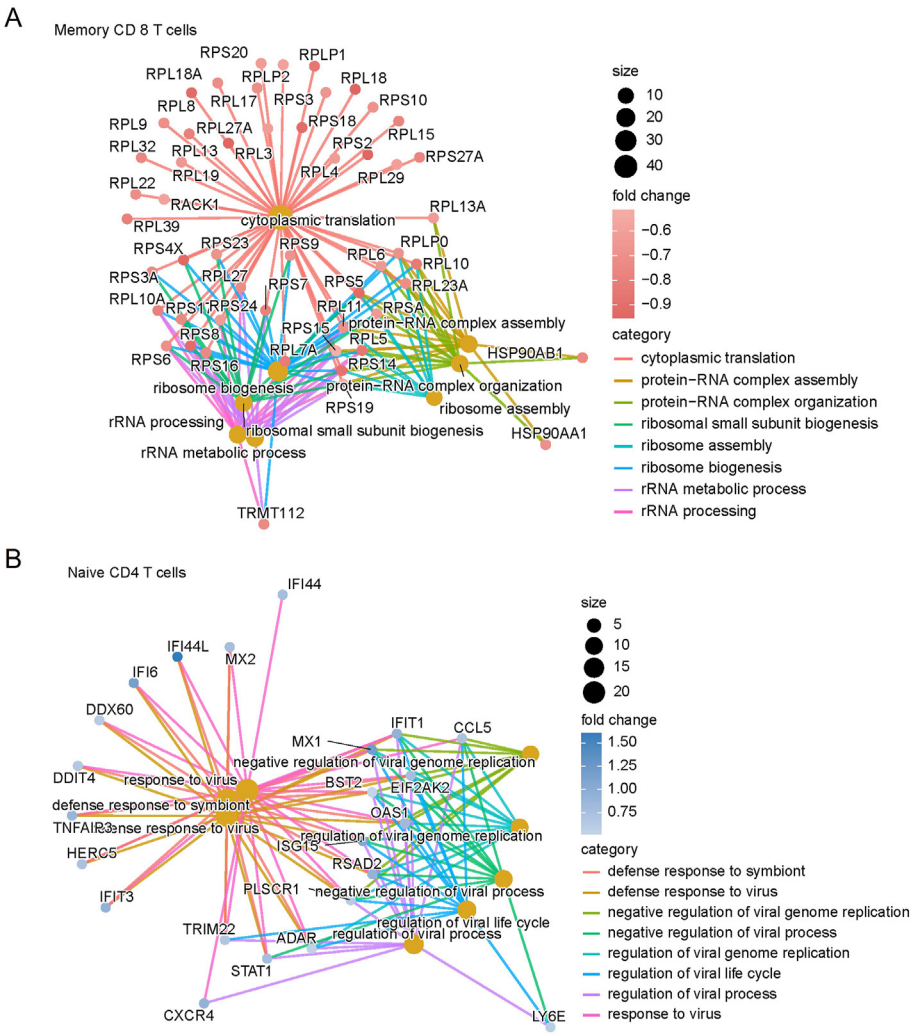

Fig. 5. HCMV infection decreased the proportion of memory CD8 T cells and naive CD4 T cells. Memory CD8 T cells and naïve CD4T cells are demonstrated The GO enrichment analysis of differential genes in the HCMV group of cells compared with the Mock group was analyzed by using clusterprofiler software to analyze the enrichment of a gene to the most significant 8 GO terms and plotted a cnetplot plot to display, the yellow dots in the graph are GO terms, the dot size represents the number of genes, the lines of different colors represent different categories, the nodes represent genes, and the color shade indicates the size of gene expression changes. **A** Memory CD8 T cell enrichment to: cytoplasmic translation, protein-RNA complex assembly, protein-RNA complex organization, ribosomal small subunit biogenesis, ribosomal assembly, ribosomal biogenesis, rRNA metabolism process, rRNA processing. **B** Naïve CD4 T cells are enriched to: defense response to symbionts, defense response to virus, negative regulation of viral genome replication, negative regulation of viral processes, regulation of viral genome replication, regulation of viral life cycle, regulation of viral processes, and response to viruses.

interaction between cell types, such as conventional cDCs, contributes to the induction of antiviral immune responses.

4. Discussion

In the current study, we provided an in-depth analysis of the single-cell dynamics of PBMCs from humanized mouse during latent and reactivated HCMV infection. Firstly, we identified 15 cell types closely associated with HCMV infection in PBMCs. Then we analyzed the changes in cell type proportions during HCMV infection. Subsequently, we performed the GO analysis on differentially expressed genes, revealing the cell types involved in host antiviral innate immune activation triggered by HCMV infection and potentially relevant genes benefiting viral immune evasion. Furthermore, we revealed a significant upregulation in cell-cell communication between different types of immune cells during HCMV infection in the humanized mice.

Humanized mice serve as valuable models for diverse biomedical researches in the recent era. In the field of infectious diseases and virus researches, humanized mice provide unique edges by studying profound immune responses in an *in vivo* and "more human" context, particularly for some viruses that specifically infect humans. These models consist of two components: immunodeficient mice and a reconstructed human immune system. The development of immunodeficient mice has undergone four stages: from Nude mice to SCID, NOD/SCID, and NOD/SCID rgnull mice, the advanced model exhibits high human cell engraftment rates, no leakage, and spontaneous thymic lymphomas (Flanagan, 1966; Priestley et al., 1998; Shultz et al., 1995; Katano et al., 2014). Based on the immunodeficient mice, engrafting human immune system components into humanized mice had various strategies. These include direct infusion of mature human immune cells, engraftment of human $CD34^{+}$ hematopoietic stem and progenitor cells (HSPCs) into immunodeficient mice followed by reconstitution with

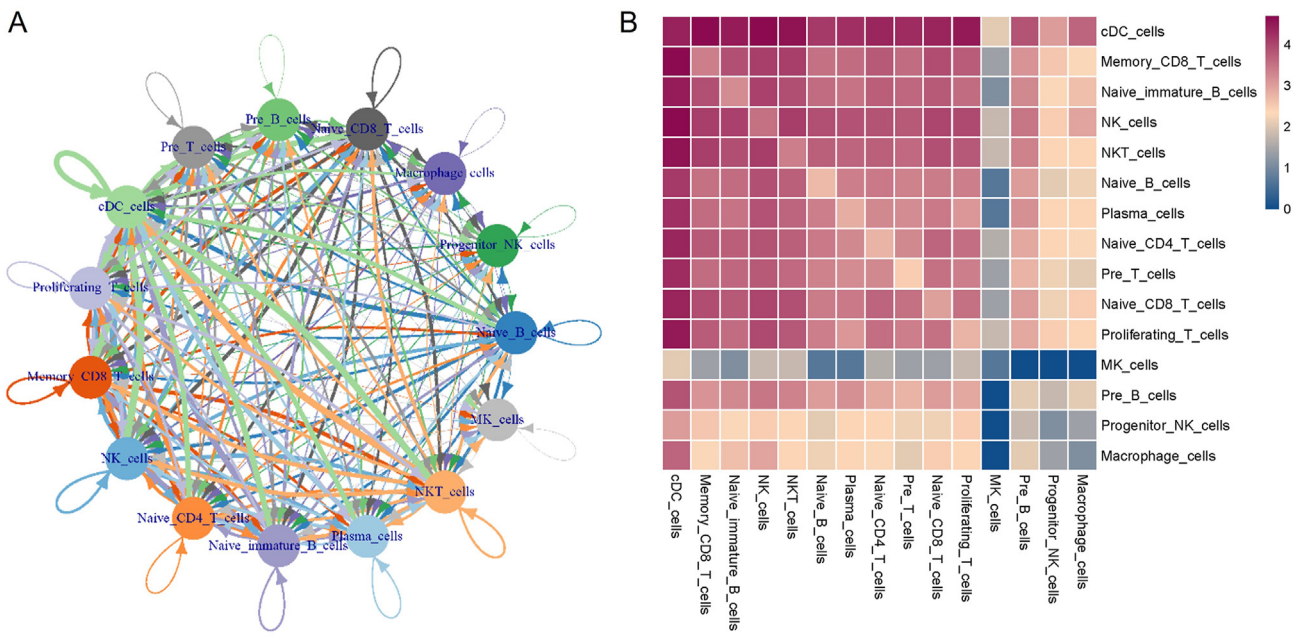

Fig. 6. HCMV infection enhanced cell-to-cell communications in humanized cells. Cell communication analysis, showing the interaction between cells between 15 cell types, based on the CellphoneDB ligand-receptor interaction database, the *P* value of a certain pair of interactions was calculated by permutation test. The cell type labels were randomly shuffled, the average expression of interactions was calculated, and the interaction pairs with *P* -value less than 0.01 were selected after 1000 repeated calculations. **A** The interaction network diagram between all cell types, the network nodes are cell types, the network edge thickness is the total logarithm of ligand and acceptor, and the line color is consistent with the ligand cell type. **B** Heat map of the number of interaction pairs between cell types, with shades of color representing the number of interaction pairs.

human SCID cells, or implantation of autologous fetal thymic tissue into SCID mice (Chuprin et al., 2023).

Due to the inherent specificity of HCMV infection and replication in human-derived cells, traditional animal models are not suitable for *in vivo* HCMV researches. On the other hand, NOD/SCID mice transplanted with huCD34 cells can effectively support systemic HCMV infection. Even after five weeks of transplantation, 52% of huCD34 cells remain detectable in peripheral blood, contributing to long-term and systemic reconstitution of multiple hematopoietic lineages and lymphocyte populations (Smith et al., 2010). This model provides a valuable platform for studying human immune responses and HCMV life cycle in an *in vivo* context.

In our research, we investigated the changes in various immune cells and their internal gene expressions in humanized mice infected with HCMV. We compared these findings with the previous reports from HCMV-infected patients. Notably, in HCMV patients, inflammatory cytokines and interferon are upregulated, which restrict pathogen spread and subsequently trigger adaptive immune responses. Stimulation of the NF-κB pathway and production of TNF-α induce dendritic cell clearance of HCMV infection. Our study revealed that most cells in the PBMCs of humanized mouse showed upregulated antiviral pathways and immune regulatory pathways following HCMV infection. Moreover, we observed that some T cells were decreased in HCMV-infected mice. Consistently, it has been reported that in septic patients with HCMV reactivation, the relative proportion of multifunctional $CD8^+$ T cells is significantly reduced (Rousselière et al., 2023). Another study conducted in a cohort of 30 HCMV-seropositive adults reported a decrease in $CD4^+$ T cells (Gabanti et al., 2014). HCMV-encoded UL10 protein has been found to impair T cell proliferation and reduce the production of pro-inflammatory cytokines in $CD4^+$ T cells (Bruno et al., 2016). Furthermore, HCMV infection significantly enhanced the cell-to-cell communications within different types of immune cells in the humanized mouse model. Therefore, our study reveals that HCMV infection effectively stimulates profound immune responses in the humanized mice, which probably resembles the human immune responses to HCMV infection, and also provides a valuable dataset for future HCMV researches.

5. Conclusions

In summary, our study employed single-cell RNA sequencing to investigate gene expression changes in PBMCs from HCMV-infected humanized mice. The robustness of this animal model for HCMV infection experiments was confirmed by our findings. These results strongly advocate for the utilization of humanized mice in HCMV research.

Data availability

The single-cell RNA-sequencing data has been deposited to Science Data Bank (CSTR: 31253.11. sciencedb.10809; DOI: 10.57760/sciencedb.10809).

Ethics statement

All animal research protocols strictly adhere to the ‘Guidelines for the Care and Use of Laboratory Animals' at the Wuhan Institute of Virology, Chinese Academy of Sciences (CAS). All experiments comply with relevant regulatory standards. The experiments and protocols have been approved by the Ethics Committee of the Wuhan Institute of Virology (WIVA24202101).

Author contributions

An Wang: formal analysis, investigation, methodology, validation, writing- original draft. Xiao-Xu Zhu: formal analysis, investigation. Yuanyuan Bie: investigation, validation. Bowen Zhang and Wenting Ji: investigation, methodology. Jing Lou: investigation, validation. Muhan Huang: formal analysis. Xi Zhou and Yujie Ren: Conceptualization,

Funding acquisition, Methodology, Supervision, Writing – original draft, Writing – review & editing.

Declaration of competing interest

Professor Xi Zhou is an editorial board member for *Virologica Sinica* and was not involved in the editorial review or the decision to publish this article. The authors of this study declared that they do not have any conflict of interest.

Acknowledgments

We are grateful to the Animal Center, Wuhan Institute of Virology, CAS, for technical assistance. We thank all members of the Zhou lab for their support.

This work was supported by the National Key R&D Program of China (2023YFC23066000 to Y.R.), the National Natural Science Foundation of China (32100106 to Y.R., and U21A20423 and 32225004 to X.Z.), the CAS Youth Innovation Promotion Association (2023351 to Y.R.), and Hubei Province Natural Science Funds (2023AFB582 to Y.R. and 2023AFA008 to X. Z), the Fund of the Science and Technology Bureau of Wuhan (2023020201010086 to Y.R.).

Appendix A. Supplementary data

Supplementary data to this article can be found online at https://doi.org/10.1016/j.virs.2024.08.006.

References

Armstrong, N., Tang, Q., 2022. Congenital cytomegalovirus infection and advances in murine models of neuropathogenesis. Virol. Sin. 37, 318–320.

Bravo, F.J., Cardin, R.D., Bernstein, D.I., 2007. A model of human cytomegalovirus infection in severe combined immunodeficient mice. Antivir. Res. 76, 104–110.

Bruno, L., Cortese, M., Monda, G., Gentile, M., Calò, S., Schiavetti, F., Zedda, L., Cattaneo, E., Piccioli, D., Schaefer, M., Notomista, E., Maione, D., Carfi, A., Merola, M., Uematsu, Y., 2016. Human cytomegalovirus pUL 10 interacts with leukocytes and impairs TCR-mediated T-cell activation. Immunol. Cell Biol. 94, 849–860.

Cho, Y.E., Lee, H., Bae, H.R., Kim, H., Yun, S., Vorn, R., Cashion, A., Rucker, M.J., Afzal, M., Latour, L., Gill, J., 2022. Circulating immune cell landscape in patients who had mild ischaemic stroke. Stroke Vasc Neurol 7, 319–327.

Chuprin, J., Buettner, H., Seedhom, M.O., Greiner, D.L., Keck, J.G., Ishikawa, F., Shultz, L.D., Brehm, M.A., 2023. Humanized mouse models for immuno-oncology research. Nat. Rev. Clin. Oncol. 20, 192–206.

Cush, S.S., Anderson, K.M., Ravneberg, D.H., Weslow-Schmidt, J.L., Flaño, E., 2007. Memory generation and maintenance of CD8+ T cell function during viral persistence. J. Immunol. 179, 141–153.

Derbois, C., Palomares, M.A., Deleuze, J.F., Cabannes, E., Bonnet, E., 2023. Single cell transcriptome sequencing of stimulated and frozen human peripheral blood mononuclear cells. Sci. Data 10, 433.

Flanagan, S.P., 1966. 'Nude', a new hairless gene with pleiotropic effects in the mouse. Genet. Res. 8, 295–309.

Fornara, C., Zavaglio, F., Furione, M., Sarasini, A., D'Angelo, P., Arossa, A., Spinillo, A., Lilleri, D., Baldanti, F., 2022. Human cytomegalovirus (HCMV) long-term shedding and HCMV-specific immune response in pregnant women with primary HCMV infection. Med. Microbiol. Immunol. 211, 249–260.

Gabanti, E., Bruno, F., Fornara, C., Bernuzzi, S., Lilleri, D., Gerna, G., 2014. Polyfunctional analysis of human cytomegalovirus (HCMV)-specific CD4(+) and CD8 (+) memory T-cells in HCMV-seropositive healthy subjects following different stimuli. J. Clin. Immunol. 34, 999–1008.

Katano, I., Ito, R., Kamisako, T., Eto, T., Ogura, T., Kawai, K., Suemizu, H., Takahashi, T., Kawakami, Y., Ito, M., 2014. NOD-Rag2null IL-2Rγnull mice: an alternative to NOG mice for generation of humanized mice. Exp. Anim. 63, 321–330.

Kealy, L., Good-Jacobson, K.L., 2021. Advances in understanding the formation and fate of B-cell memory in response to immunization or infection. Oxf Open Immunol 2, iqab018.

Klenerman, P., Oxenius, A., 2016. T cell responses to cytomegalovirus. Nat. Rev. Immunol. 16, 367–377.

Kugelberg, E., 2015. B cell memory: making sense in humans. Nat. Rev. Immunol. 15, 133.

Liao, J., Qian, J., Fang, Y., Chen, Z., Zhuang, X., Zhang, N., Shao, X., Hu, Y., Yang, P., Cheng, J., Hu, Y., Yu, L., Yang, H., Zhang, J., Lu, X., Shao, L., Wu, D., Gao, Y., Chen, H., Fan, X., 2022. De novo analysis of bulk RNA-seq data at spatially resolved single-cell resolution. Nat. Commun. 13, 6498.

Peng, O., Wei, X., Ashraf, U., Hu, F., Xia, Y., Xu, Q., Hu, G., Xue, C., Cao, Y., Zhang, H., 2022. Genome-wide transcriptome analysis of porcine epidemic diarrhea virus virulent or avirulent strain-infected porcine small intestinal epithelial cells. Virol. Sin. 37, 70–81.

Priestley, A., Beamish, H.J., Gell, D., Amatucci, A.G., Muhlmann-Diaz, M.C., Singleton, B.K., Smith, G.C., Blunt, T., Schalkwyk, L.C., Bedford, J.S., Jackson, S.P., Jeggo, P.A., Taccioli, G.E., 1998. Molecular and biochemical characterisation of DNA-dependent protein kinase-defective rodent mutant irs-20. Nucleic Acids Res. 26, 1965–1973.

Ramírez-Sánchez, A.D., Chu, X., Modderman, R., Kooy-Winkelaar, Y., Koletzko, S., Korponay-Szabó, I.R., Troncone, R., Wijmenga, C., Mearin, L., Withoff, S., Jonkers, I.H., Li, Y., 2022. Single-cell RNA sequencing of peripheral blood mononuclear cells from pediatric coeliac disease patients suggests potential pre-seroconversion markers. Front. Immunol. 13, 843086.

Ren, Y., Wang, A., Wu, D., Wang, C., Huang, M., Xiong, X., Jin, L., Zhou, W., Qiu, Y., Zhou, X., 2022. Dual inhibition of innate immunity and apoptosis by human cytomegalovirus protein UL37x1 enables efficient virus replication. Nat Microbiol 7, 1041–1053.

Rousselière, A., Delbos, L., Foureau, A., Reynaud-Gaubert, M., Roux, A., Demant, X., Le Pavec, J., Kessler, R., Mornex, J.F., Messika, J., Falque, L., Le Borgne, A., Boussaud, V., Tissot, A., Hombourger, S., Bressollette-Bodin, C., Charreau, B., 2023. Changes in HCMV immune cell frequency and phenotype are associated with chronic lung allograft dysfunction. Front. Immunol. 14, 1143875.

Shang, Q.N., Yu, X.X., Xu, Z.L., Chen, Y.H., Han, T.T., Zhang, Y.Y., Lv, M., Sun, Y.Q., Wang, Y., Xu, L.P., Zhang, X.H., Zhao, X.Y., Huang, X.J., 2023. Expanded clinical-grade NK cells exhibit stronger effects than primary NK cells against HCMV infection. Cell. Mol. Immunol. 20, 895–907.

Shnayder, M., Nachshon, A., Rozman, B., Bernshtein, B., Lavi, M., Fein, N., Poole, E., Avdic, S., Blyth, E., Gottlieb, D., Abendroth, A., Slobedman, B., Sinclair, J., Stern-Ginossar, N., Schwartz, M., 2020. Single cell analysis reveals human cytomegalovirus drives latently infected cells towards an anergic-like monocyte state. Elife 9, e52168.

Shultz, L.D., Schweitzer, P.A., Christianson, S.W., Gott, B., Schweitzer, I.B., Tennent, B., Mckenna, S., Mobraaten, L., Rajan, T.V., Greiner, D.L., et al., 1995. Multiple defects in innate and adaptive immunologic function in NOD/LtSz-scid mice. J. Immunol. 154, 180–191.

Smith, M.S., Goldman, D.C., Bailey, A.S., Pfaffle, D.L., Kreklywich, C.N., Spencer, D.B., Othieno, F.A., Streblow, D.N., Garcia, J.V., Fleming, W.H., Nelson, J.A., 2010. Granulocyte-colony stimulating factor reactivates human cytomegalovirus in a latently infected humanized mouse model. Cell Host Microbe 8, 284–291.

Stuart, T., Satija, R., 2019. Integrative single-cell analysis. Nat. Rev. Genet. 20, 257–272.

Zabalza, A., Vera, A., Alari-Pahissa, E., Munteis, E., Moreira, A., Yélamos, J., Llop, M., López-Botet, M., Martínez-Rodríguez, J.E., 2020. Impact of cytomegalovirus infection on B cell differentiation and cytokine production in multiple sclerosis. J. Neuroinflammation 17, 161.

Zehner, M., Alt, M., Ashurov, A., Goldsmith, J.A., Spies, R., Weiler, N., Lerma, J., Gieselmann, L., Stöhr, D., Gruell, H., Schultz, E.P., Kreer, C., Schlachter, L., Janicki, H., Laib Sampaio, K., Stegmann, C., Nemetchek, M.D., Dähling, S., Ullrich, L., Dittmer, U., Witzke, O., Koch, M., Ryckman, B.J., Lotfi, R., Mclellan, J.S., Krawczyk, A., Sinzger, C., Klein, F., 2023. Single-cell analysis of memory B cells from top neutralizers reveals multiple sites of vulnerability within HCMV Trimer and Pentamer. Immunity 56, 2602–2620.e10.